ANTIMICROBIAL AGENTS AND CHEMOTHERAPY, Apr. 2004, p. 1335–1343 Vol. 48, No. 4
0066-4804/04/$08.00+0 DOI: 10.1128/AAC.48.4.1335–1343.2004

Potent Synergistic In Vitro Interaction between Nonantimicrobial Membrane-Active Compounds and Itraconazole against Clinical Isolates of *Aspergillus fumigatus* Resistant to Itraconazole

Javier Afeltra,[1,2] Roxana G. Vitale,[1,2] Johan W. Mouton,[3] and Paul E. Verweij[1,2]*

Department of Medical Microbiology, University Medical Center Nijmegen,[1] Department of Medical Microbiology and Infectious Diseases, Canisius Wilhemina Hospital,[3] and Nijmegen University Center for Infectious Diseases,[2] Nijmegen, The Netherlands

Received 30 June 2003/Returned for modification 24 August 2003/Accepted 12 November 2003

To develop new approaches for the treatment of invasive infections caused by *Aspergillus fumigatus*, the in vitro interactions between itraconazole (ITZ) and seven different nonantimicrobial membrane-active compounds—amiodarone (AMD), amiloride, lidocaine, lansoprazole (LAN), nifedipine (NIF), verapamil, and fluphenazine—against seven ITZ-susceptible and seven ITZ-resistant (ITZ-R) strains were evaluated by the checkerboard microdilution method based on National Committee for Clinical Laboratory Standards M-38A guidelines. The nature and the intensity of the interactions were assessed by a nonparametric approach (fractional inhibitory concentration [FIC] index model), a fully parametric response surface approach (Greco model) of the Loewe additivity no-interaction theory, and the nonparametric (Prichard model) and semiparametric response surface approaches of the Bliss independence (BI) no-interaction theory. Statistically significant synergy was found for the combination of ITZ and AMD and the combination of LAN and NIF, although with different intensities against ITZ-R strains. The FIC index values ranged from 1 to 0.02 for ITZ-AMD, 0.53 to 0.04 for ITZ-LAN, and 0.28 to 0.06 for ITZ-NIF. By use of the BI-based model, the strongest synergy was found for the combination of ITZ with AMD, followed by the combination of ITZ and NIF. The parametric models could not be fit adequately because most of the drugs alone did not show any effect and, thus, no sigmoid dose-response. In general, the combination of ITZ with calcium pump blockers displayed in vitro synergistic activity, primarily against ITZ-R strains, and warrants further investigation.

Invasive aspergillosis causes approximately 30% of invasive fungal infections in patients treated for cancer (11). Until 1990 only one drug was available for the treatment of invasive *Aspergillus* disease, amphotericin B, which must be given intravenously and which has a number of serious toxicities. In 1990 itraconazole (ITZ) capsules became available and *Aspergillus* species were included in the spectrum of activity of the drug, although the drug was mainly used in the prophylactic setting due to poor bioavailability (11). Ten years later an intravenous formulation of ITZ became available and allowed the drug to be used for the empirical or preemptive treatment of high-risk patients. With the registration of voriconazole and caspofungin, the arsenal of available drugs has increased further. However, despite antifungal therapy, the rate of mortality in patients with invasive aspergillosis remains very high, and clearly, new therapeutic approaches are needed. Combination therapy is one approach that can be used to improve the efficacy of antimicrobial therapy for difficult-to-treat infections, such as human immunodeficiency virus and mycobacterial infections. By analogy, the combination of ITZ with other compounds could represent a possible approach for the treatment of patients with invasive aspergillosis or patients infected with strains with reduced susceptibilities to antifungal agents. Resistance to antifungal azoles has been studied in yeasts and molds, especially *Aspergillus*. Resistance mechanisms include changes in the cellular azole content (an altered uptake or efflux mechanism), mutations in sterol desaturation during ergosterol biosynthesis, and mutations in or elevated levels of 14α-demethylase (12, 42). The recent discovery of drug efflux-mediated resistance mechanisms in yeasts and *Aspergillus* opens new therapeutic concepts. It has been recognized that *Candida albicans* and *Aspergillus nidulans* express multidrug efflux transporter (MET) genes belonging to different classes, i.e., the ATP-binding cassette (ABC) transporters and the major facilitators (13, 48). The expression of these genes and their targeted deletion determine the level of azole resistance.

In this study we investigated the in vitro interactions between ITZ and different nonantimicrobial membrane-active compounds against clinical ITZ-resistant (ITZ-R) and ITZ-susceptible (ITZ-S) strains using four different drug interaction models.

MATERIALS AND METHODS

Strains. Fourteen clinical isolates of *Aspergillus fumigatus* were tested. These included seven ITZ-S isolates (isolates V09-22, V09-23, AZN5161, AZN7820, AZN8248, AZN9339, and AZN9362) and seven ITZ-R isolates (isolates V09-18, V09-19, AZN5241, AZN5242, AZN7720, AZN7722, and AZG7). The strains numbered AZN and V09 were obtained from the private collection of the Department of Medical Microbiology, University Medical Center Nijmegen, and strain AZG7 was obtained from the University Hospital Groningen, Groningen, The Netherlands (52). All isolates were subcultured on potato dextrose agar for 5 to 7 days at 30°C.

Quality controls. *Candida parapsilosis* (ATCC 22019) and *Candida krusei* (ATCC 6815) were used as quality control strains.

* Corresponding author. Mailing address: Department of Medical Microbiology, University Medical Center Nijmegen, P.O. Box 9101, 6500 HB Nijmegen, The Netherlands. Phone: 31-24-3614356. Fax: 31-24-3540216. E-mail: p.verweij@mmb.umcn.nl.

Inoculum preparation. Conidia of the isolates were obtained from fresh cultures for the preparation of each inoculum. Spores were collected with a cotton stick and suspended in sterile water. After the heavy particles were allowed to settle, the turbidities of the supernatants were measured spectrophotometrically (Spectronic 20D; Milton Roy, Rochester, N.Y.) at 530 nm, the transmission was adjusted to 80 to 82%, and the supernatants were diluted to obtain a final inoculum of 0.4×10^4 to 5×10^4 CFU/ml. The inoculum size was verified by determination of the number of viable CFU after serial dilutions of the inoculum were plated onto Sabouraud dextrose agar.

Drugs used. All solutions were prepared ex novo with powders from the same lot. The drugs used in this study were ITZ (Janssen-Cilag, Tilburg, The Netherlands) and amiloride (AML), amiodarone (AMD), fluphenazine (FLU), lansoprazole (LAN), lidocaine (LID), nifedipine (NIF), and verapamil (VER), all from Sigma-Aldrich Chemie GmbH, Steinheim, Germany. The final concentrations of the drugs ranged from 0.03 to 16 μg/ml for ITZ, 0.13 to 8 μg/ml for AMD and AML, 1.25 to 80 μg/ml for FLU and NIF, 0.6 to 40 μg/ml for LAN, 0.25 to 16 μg/ml for LID, and 10 to 640 μg/ml for VER. All drugs were dissolved in dimethyl sulfoxide as the solvent. The concentrations of the membrane-active drugs were chosen to be within the range achievable in human plasma and were also those used in previous studies (1–3, 9, 17, 22, 31, 32, 38).

MICs. MICs were determined by a broth microdilution method described in National Committee for Clinical Laboratory Standards (NCCLS) guidelines (M-38A) (43).

The drug dilutions were made in RPMI 1640 medium (with L-glutamine, without bicarbonate; GIBCO BRL, Life Technologies, Woerden, The Netherlands) buffered to pH 7.0 with 0.165 morpholinepropanesulfonic acid (Sigma-Aldrich Chemie GmbH, Steinheim, Germany). The test was performed in 96-well flat-bottom microtitration plates, which were kept at −70°C until the day of testing. Each suspension of spores was diluted 1:50 in RPMI 1640 medium to obtain two times the desired inoculum.

Growth was graded on a scale from 0 to 4, as follows: 4 indicated no reduction in growth, 3 indicated a 25% reduction of growth, 2 indicated a 50% reduction of growth, 1 indicated a 75% reduction of growth, and 0 indicated an optically clear well. The MIC endpoint was defined as the lowest concentration of the drugs (alone or in combination) showing 50% inhibition of growth compared with that of the drug-free control (MIC-2). After agitation, the plates were incubated at 35°C for 48 h, after which the optical density (OD) was measured with a spectrophotometer (MS2 reader, Titertek-plus; ICN Biomedical Ltd., Basingstoke, United Kingdom) at 405 nm. The OD of the blank, to which a conidium-free inoculum had been added, was subtracted from the OD values. The percentage of growth for each well was calculated by comparing the OD of the drug-containing well with that of the drug-free control well.

Drug interactions. The in vitro interactions between ITZ and the blockers were studied by a two-dimensional checkerboard microdilution technique in sterile, 96-well flat-bottom microtitration plates, as described below. Each isolate was tested three times on different days.

(i) Microtitration plate setup. For the combination studies, each drug was first serially diluted twofold in the corresponding solvents and then 100-fold in the medium, according to the dilution scheme of NCCLS for water-insoluble drugs, in order to obtain four times the final concentration. A total of 50 μl of each concentration of the azole was added to columns 1 to 10, and then 50 μl of each concentration of the corresponding blocker was added to rows A to G. Column 12 was the drug-free well that served as the growth control.

Drug interaction modeling. In order to assess the nature of the in vitro interaction between the drugs, the data obtained were analyzed by using four different models that have successfully been used to characterize antifungal drug interactions (18, 39, 53). The models were parametric and nonparametric approaches of the following two no-interaction theories: the Loewe additivity and the Bliss independence (BI) theories. In the Loewe additivity theory the concentrations of the drugs, alone or in combination, that produce the same effect are compared, while in the BI-based models, the estimates of the combined effect based on the effects of the individual drugs were compared with those obtained in the experiment.

(i) Loewe additivity. Loewe additivity is described by the following equation: $1 = d_A/D_A + d_B/D_B$, where d_A and d_B are the concentrations of drugs A and B in the combination which elicit a certain effect, respectively, and D_A and D_B are the isoeffective concentrations of drugs A and B acting alone, respectively. The nonparametric approach is based on the fractional inhibitory concentration (FIC) index (FICI), which is expressed by the following equation:

$$\sum \mathrm{FIC} = \mathrm{FIC}_A + \mathrm{FIC}_B = \frac{C_A^{\mathrm{comb}}}{\mathrm{MIC}_A^{\mathrm{alone}}} + \frac{C_B^{\mathrm{comb}}}{\mathrm{MIC}_B^{\mathrm{alone}}}$$

where $\mathrm{MIC}_A^{\mathrm{alone}}$ and $\mathrm{MIC}_B^{\mathrm{alone}}$ are the concentrations of drugs A and B acting alone, respectively, and C_A^{comb} and C_B^{comb} are the concentrations of drugs A and B at the isoeffective combinations, respectively (21). Off-scale MICs were converted to the next highest or the next lowest doubling concentration. For each data set, $\Sigma\mathrm{FIC}_{\mathrm{min}}$ (where min is minimum) was determined when $\Sigma\mathrm{FIC}_{\mathrm{max}}$ (where max is maximum) was less than 4; otherwise $\Sigma\mathrm{FIC}_{\mathrm{max}}$ was determined (21).

The interpretation of the FICI was as follows: synergistic effect, FICI ≤ 0.5; no interaction, FICI > 0.5 but ≤ 4; and antagonistic effect, FICI > 4 (44). In practice, synergy or antagonism calculated in this way is equivalent to a reduction or an increase, respectively, of at least 2 dilutions steps in the MIC of the combination compared to the MICs of the drugs alone.

The fully parametric surface approach described by Greco et al. (18) was used based on the following equation:

$$1 = \frac{D_A}{\mathrm{IC}_{50,A}\left(\frac{E}{E_{\max} - E}\right)^{1/m_A}} + \frac{D_B}{\mathrm{IC}_{50,B}\left(\frac{E}{E_{\max} - E}\right)^{1/m_B}} + \alpha\frac{D_A D_B}{\mathrm{IC}_{50,A}\mathrm{IC}_{50,B}\left(\frac{E}{E_{\max} - E}\right)^{0.5(1/m_A + 1/m_B)}}$$

where E is the OD (dependent variable) at drug concentrations D_A and D_B (independent variables); $E_{\max}$ is the maximal OD observed for the drug-free control; $\mathrm{IC}_{50,A}$ and $\mathrm{IC}_{50,B}$ are the drug concentrations producing 50% of the $E_{\max}$ for drugs A and B, respectively; m_A and m_B are the slopes of the concentration-effect curves (Hill coefficient) for drugs A and B, respectively; and α is the interaction parameter which describes the nature of the interaction. This model was fitted directly to experimental data (the average OD among the replicates for all concentrations of the two drugs alone or in combination) by a nonweighted, nonlinear regression analysis with the MODLAB program (www.medimatics.nl; MEDIMATICS, Maastricht, The Netherlands). Goodness-of-fit criteria included the 95% confidence interval (CI) of the fitted parameters, R^2, the sum of squares, correlation and covariance matrices, and the residual plots.

When the parameter α as well as its 95% CI was positive statistically significant, synergy was claimed, while when α as well as its 95% CI was negative statistically, significant antagonism was claimed. In any other case, Loewe additivity was concluded. The additivity surface was simulated by fixing all parameters of the Greco model except α to the values obtained after the model was fitted to experimental data; α was fixed at 0. The fitted experimental surface calculated by the Greco model was then subtracted from the additivity surface calculated as described above.

(ii) BI. BI is described by the equation $I_i = (I_A + I_B) - (I_A \times I_B)$, where I_i is the predicted percentage of inhibition of the theoretical combination of drugs A and B, and I_A and I_B are the experimental percentages of inhibition of each drug acting alone, respectively. Since I is equal to $1 - E$, where E is the percentage of growth, and by substitution into the former equation, the following equation is derived: $E_i = E_A \times E_B$, where E_i is the predicted percentage of growth of the theoretical combination of drugs A and B, respectively, and E_A and E_B are the experimental percentages of inhibition and growth of each drug acting alone, respectively. Interaction is described by the difference ΔE between the predicted and the measured percentages of growth at various concentrations. Because of the nature of the interaction, testing with microtiter plates and a twofold dilution of either drug results in a ΔE for each drug combination. A surface plot is obtained by use of a three-dimensional plot, with ΔE depicted on the z axis. By the nonparametric surface approach described by Prichard and colleagues (46, 47), E_A and E_B are obtained directly from the experimental data, while by the semiparametric surface approach (14, 18), these values are derived from fitting of the $E_{\max}$ model to the concentration-effect curve for each drug alone. Thus, for the latter approach, E_A and E_B are obtained by the following equation: $E_{A,B} = E_{\max} \times (D/\mathrm{IC}_{50})^m/[1 + (D/\mathrm{IC}_{50})^m]$, where E, D, $E_{\max}$, IC_{50}, and m are the same parameters for drugs A and B described above. The parameters of the model were obtained by a nonweighted nonlinear regression analysis with GraphPad Prism software (San Diego, Calif.). Data were normalized by using the percentages; and the maximum and the minimum values of the $E_{\max}$ model, corresponding to 100% and 0%, respectively, were kept constant. The fit of the model was interpreted by using the run test and the R^2 values. After the $E_{\max}$ model was fitted to the data, the parameters generated were used to calculate the no-interaction surface for each replicate separately.

For each combination of two drugs in each of the three independent experiments, the observed OD of growth obtained from the experimental data was subtracted from the predicted OD, calculated as described above for each model.

TABLE 1. In vitro interaction between ITZ and AMD[a]

Strain	MIC (μg/ml) alone		Result according to theory						
			LA				BI (nonparametric)		
			MIC (μg/ml) in combination		Result				
	ITZ	AMD	ITZ	AMD	FICI	INT	ΣSYN (*n*)	ΣANT (*n*)	INT
V09-22	0.12	16	0.06	0.25	0.52	NI	7 (5)	−1.2 (1)	NI
V09-23	0.12	16	0.12	0.25	1	NI	3.6 (4)	−1.3 (2)	NI
AZN-5161	0.12	16	0.12	0.12	1	NI	4.2 (5)	−1.1 (1)	NI
AZN-7820	0.12	16	0.06	0.12	0.51	NI	44.3 (4)	−24.6 (2)	NI
AZN-8248	0.12	16	0.12	0.12	1	NI	38.4 (5)	−6.7 (2)	NI
AZN-9339	0.25	16	0.12	0.25	0.5	SYN	37.1 (4)	−1.4 (2)	NI
AZN-9362	0.25	16	0.12	0.12	0.5	SYN	26.6 (15)	−3.2 (4)	NI
Median	0.12	16			0.52		26.6	−1.4	
V09–18	32	16	0.12	0.25	0.02	SYN	476 (40)	−38 (15)	SYN
V09–19	32	16	1	0.25	0.05	SYN	600 (35)	−34.2 (5)	SYN
AZN-5241	32	16	2	0.5	0.09	SYN	1,482 (50)	−7.1 (1)	SYN
AZN-5242	32	16	16	8	1	NI	930 (56)	−37.9 (10)	SYN
AZN-7720	32	16	0.25	0.5	0.04	SYN	108 (30)	−10.1 (2)	SYN
AZN-7722	32	16	2	2	0.19	SYN	678 (53)	−42.9 (10)	SYN
AZG7	32	16	8	4	0.5	SYN	122 (30)	−8.48 (9)	SYN
Median	32	16			0.09		600	−34.2	

[a] Abbreviations: LA, Loewe additivity; INT, interpretation; NI, no interaction; SYN, synergism; ANT, antagonism; *n*, number of interactions.

When the average difference as well as its 95% CI among the four replicates was positive, statistically significant synergy was claimed; when the difference as well as its 95% CI was negative, significant antagonism was claimed. In any other case, BI was concluded. The values thus obtained for each combination were used to construct a three-dimensional plot. Peaks above and below the 0 plane indicate synergistic and antagonistic combinations, respectively, while the 0 plane indicates no statistically significant interaction. The contour plots were also constructed in order to visualize the drug concentrations that produce an interaction.

Since the plot shows only the interactions for each separate combination of the concentrations, a value is needed to summarize the interaction surface. This was done by calculating the sums of the percentages of all statistically significant synergistic (ΣSYN) and antagonistic (ΣANT) interactions. Interactions with <100% statistically significant interactions were considered weak, interactions with 100 to 200% statistically significant interactions were considered moderate, and interactions with >200% statistically significant interactions were considered strong, as described previously (39). In addition, the numbers of statistically significant synergistic and antagonistic combinations among the 96 combinations of drug concentrations tested were calculated for each strain.

RESULTS

The MICs of ITZ, based on a 50% reduction of growth, for *C. krusei* (ATCC 6815) and *C. parapsilosis* (ATCC 22019) were 0.5 and 0.25 μg/ml, respectively, which are within the reference range for quality control strains for ITZ. No reference range has been established for the other drugs. Nevertheless, none of the blocker drugs alone appeared to be active against the *Candida* isolates. The final inoculum varied from 1.5×10^4 to 4×10^4 CFU/ml. The MIC of ITZ ranged from 16 to 32 μg/ml for the ITZ-R *A. fumigatus* isolates and from 0.12 to 0.25 μg/ml for the ITZ-S isolates. AMD, AML, LAN, LID, and VER were inactive in vitro against all strains tested. However, NIF and FLU were active against some strains, with geometric mean MICs of 15 μg/ml (range, 5 to 80 μg/ml) and 51 μg/ml (range, 10 to 160 μg/ml), respectively.

Drugs in combination. (i) FICI evaluation and BI model. (a) ITZ plus AMD. ITZ and AMD displayed no interaction against most of the ITZ-S *A. fumigatus* strains tested but were synergistic against two strains. However, the combination was synergistic against six of the ITZ-R strains, with the FICIs ranging from 0.02 to 1. By the BI method all ITZ-S strains displayed very low percentages of synergistic and antagonistic interactions, ranging between 3.6 and 44.3% and −1.1 and −24.6%, respectively. Synergistic interactions predominated against the ITZ-R strains, with from 108 to 1,482% synergistic interactions and −42.9 to −7.1% antagonistic interactions (Table 1 and Fig. 1).

(b) ITZ plus AML. ITZ and AML were synergistic against two ITZ-S *A. fumigatus* strains, with FICIs ranging from 0.5 to 1, and against five strains by use of the BI model, with variations ranging from 219.16 to 52.7% for synergistic interactions and −10.6 to −89.4% for antagonistic interactions. A synergistic interaction against three ITZ-R strains was displayed by use of the FICI and against five isolates by use of the BI model (data not shown).

(c) ITZ plus LAN. The interaction between ITZ and LAN against the ITZ-S *A. fumigatus* strains was less synergistic than that against the ITZ-R *A. fumigatus* strains, with FICIs ranging from 0.15 to 0.75; by use of the BI model, the drugs displayed synergistic interactions against only three to seven strains. On the contrary, the combination was more synergistic against the ITZ-R strains by both methods evaluated (Table 2).

(d) ITZ plus LID. In general, the combination of ITZ and LID displayed no interaction against ITZ-S strains according to the FICIs (range, 0.5 to 1), whereas moderate synergistic interactions were found against the ITZ-R strains according to the FICIs (range, 0.02 to 1) and also when the BI model was used to characterize the interaction (Fig. 2).

(e) ITZ plus NIF. The combination of ITZ and NIF showed synergistic effects against some ITZ-S isolates by both methods. On the contrary, the combination showed potent synergistic interactions against ITZ-R strains in both models, with

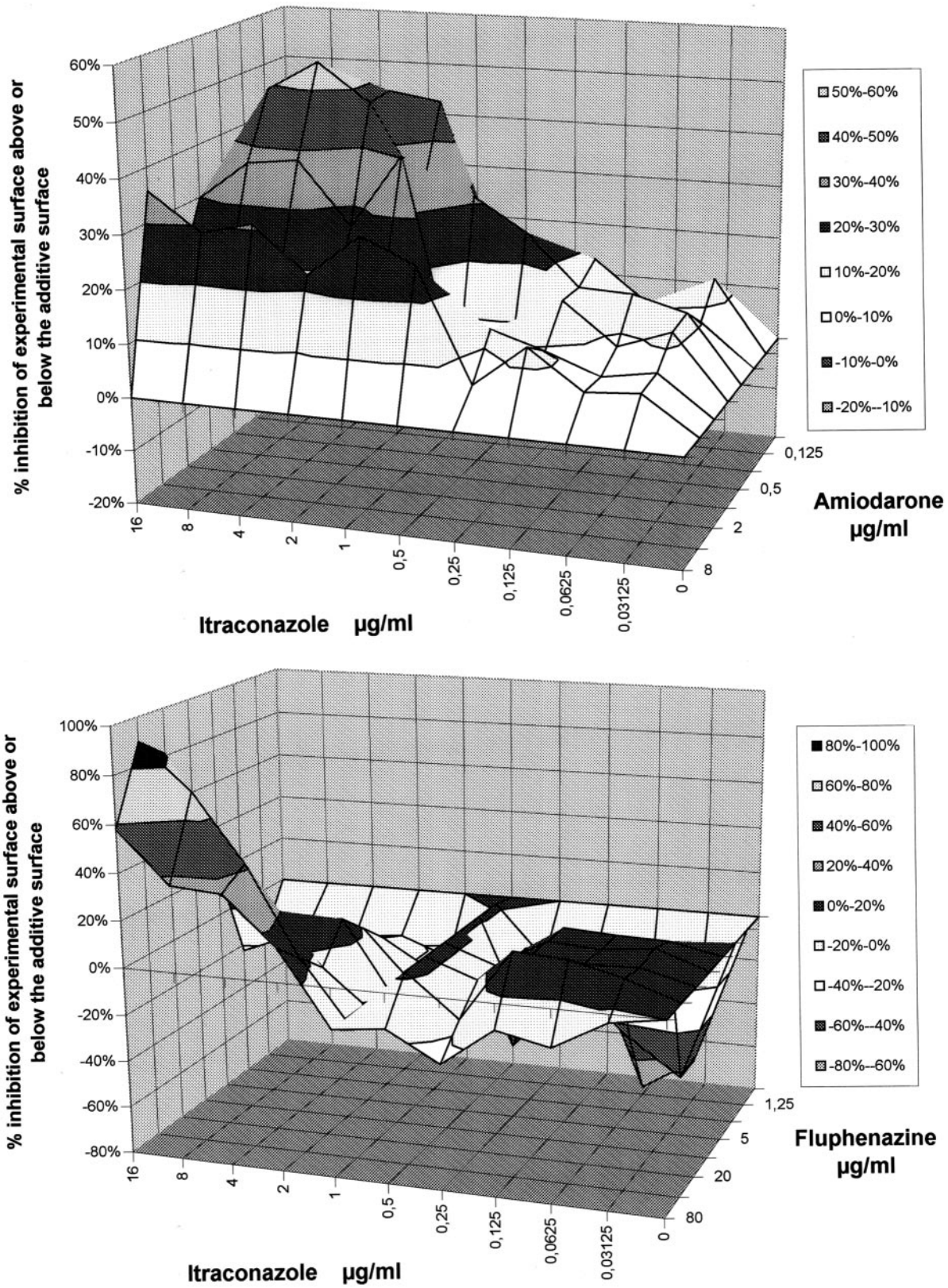

FIG. 1. Assessment of in vitro interactions based on the BI theory. (A) Three-dimensional graph of the synergy of ITZ and AMD in combination against an ITZ-R strain calculated by the nonparametric approach; (B) three-dimensional graph of the synergy-antagonism of ITZ and FLU in combination against an ITZ-R strain calculated by the nonparametric approach.

TABLE 2. In vitro interaction between ITZ and LAN[a]

Strain	MIC (μg/ml) alone		Result according to theory						
			LA				BI (nonparametric)		
			MIC (μg/ml) in combination		Result				
	ITZ	LAN	ITZ	LAN	FICI	INT	ΣSYN (*n*)	ΣANT (*n*)	INT
V09-22	0.12	80	0.06	20	0.75	NI	97.5 (13)	−75.8 (14)	NI
V09-23	0.25	80	0.12	2.5	0.51	NI	87.4 (8)	−13.4 (2)	NI
AZN-5161	0.12	80	0.06	20	0.75	NI	147 (16)	−86.3 (4)	SYN
AZN-7820	0.12	80	0.06	10	0.63	NI	97.8 (20)	−13.9 (7)	NI
AZN-8248	0.12	80	0.06	20	0.75	NI	35.7 (1)	−53.6 (4)	NI
AZN-9339	0.25	80	0.03	2.5	0.15	SYN	134 (24)	−12.7 (8)	SYN
AZN-9362	0.25	80	0.06	5	0.18	SYN	112 (9)	−93.2 (12)	SYN
Median	0.12	80			0.63		97.8	−53.6	
V09-18	32	80	0.12	5	0.07	SYN	216 (16)	−11.6 (5)	SYN
V09-19	32	80	0.25	2.5	0.04	SYN	378 (21)	−46.4 (2)	SYN
AZN-5241	32	80	1	40	0.53	NI	119 (11)	−38.1 (9)	SYN
AZN-5242	32	80	1	20	0.28	SYN	301 (19)	−28.3 (4)	SYN
AZN-7720	16	80	0.12	20	0.26	SYN	119 (10)	−16.1 (2)	SYN
AZN-7722	32	80	1	2.5	0.06	SYN	209 (18)	−21.4 (8)	SYN
AZG7	16	80	0.5	2.5	0.06	SYN	162 (13)	−30.7 (2)	SYN
Median	32	80			0.07		209	−28.3	

[a] Abbreviations: LA, Loewe additivity; INT, interpretation; NI, no interaction; SYN, synergism; ANT, antagonism; *n*, number of interactions.

FICIs ranging from 0.06 to 0.28 and with the values from the BI model ranging from 134.26 to 1114.9% (Table 3).

(f) ITZ plus FLU. The combination of ITZ and FLU had a synergistic effect against only three ITZ-R strains, whereas no interaction against the other strains was indicated by use of FICI. In contrast, by use of the BI model, the interactions of the combination varied between synergistic and antagonistic against all the strains, resulting in statistically significant differences (Table 4 and Fig. 1).

(g) ITZ plus VER. By use of FICI the combination of ITZ and VER had no interaction against most of the strains. In contrast, by use of the BI model the combination was synergistic against four ITZ-S strains and varied between synergistic and antagonistic against the ITZ-R strains (data no shown).

In general, when conventional antifungal agents were combined with pump blockers, relatively high FICIs (>0.5) were observed against ITZ-R strains, whereas lower FICIs (0.02 to 1) were found against ITZ-R strains.

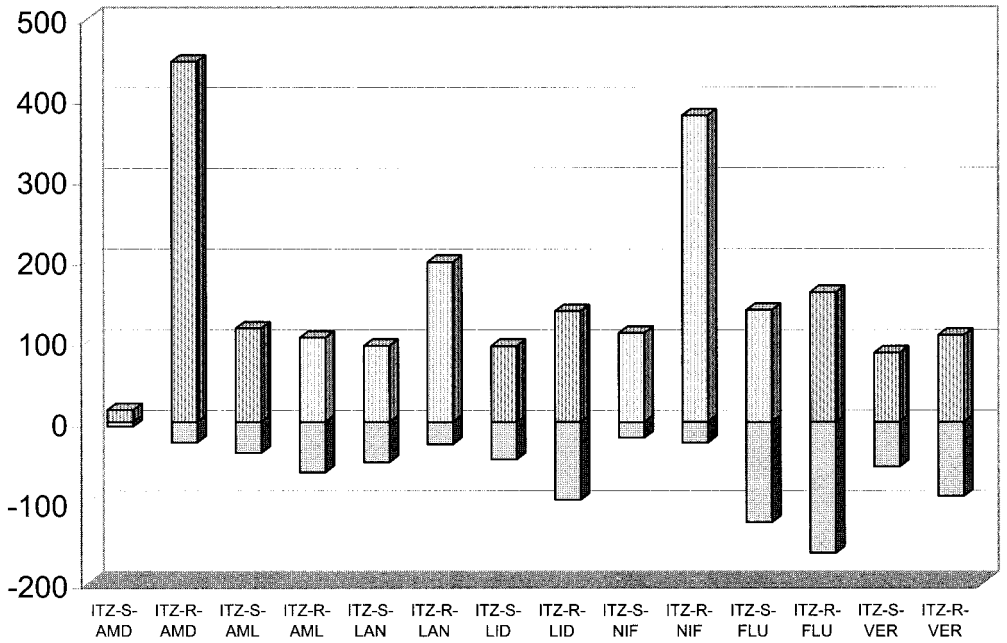

FIG. 2. Comparison of the activities of all drugs against ITZ-S and ITZ-R *A. fumigatus* strains by using the BI model.

TABLE 3. In vitro interaction between ITZ and NIF[a]

Strain	MIC (μg/ml) alone		Result according to theory						
			LA				BI (nonparametric)		
			MIC (μg/ml) in combination		Result				
	ITZ	NIF	ITZ	NIF	FICI	INT	ΣSYN (*n*)	ΣANT (*n*)	INT
V09-22	0.25	10	0.12	1.2	0.6	NI	511 (15)	−21.5 (7)	SYN
V09-23	0.25	20	0.03	5	0.35	SYN	45.3 (19)	−9.2 (4)	NI
AZN5161	0.12	10	0.03	5	0.75	NI	60.6 (12)	−25.7 (1)	NI
AZN7820	0.25	5	0.06	1.25	0.50	SYN	321.6 (11)	−62.9 (8)	SYN
AZN8248	0.25	10	0.06	2.5	0.50	SYN	232 (27)	−10.8 (3)	SYN
AZN9339	0.25	10	0.12	2.5	0.75	NI	45.3 (12)	0 (0)	NI
AZN9362	0.25	20	0.03	2.5	0.25	SYN	42.2 (30)	−6.9 (10)	NI
Median	0.25	10			0.5		60.6	−10.8	
V09-18	32	10	1	1.2	0.15	SYN	218 (35)	−21.2 (1)	SYN
V09-19	32	10	1	1.2	0.15	SYN	219 (13)	0 (0)	SYN
AZN5241	32	10	1	2.5	0.28	SYN	552 (24)	−66.7 (3)	SYN
AZN5242	32	80	1	2.5	0.06	SYN	1050 (18)	0 (0)	SYN
AZN7720	16	80	0.25	10	0.14	SYN	134 (41)	−1.5 (1)	SYN
AZN7722	32	10	1	1.2	0.15	SYN	1,114 (38)	−72.6 (5)	SYN
AZG7	32	20	1	2.5	0.16	SYN	272 (14)	−16.9 (3)	SYN
Median	32	10			0.15		272	−16.9	

[a] Abbreviations: LA, Loewe additivity; INT, interpretation; NI, no interaction; SYN, synergism; ANT, antagonism; *n*, number of interactions.

By use of the BI model and the assumption of a limit of a 100% interaction, the highest synergistic interaction was observed for ITZ and AMD, followed by ITZ and NIF, against ITZ-R strains. Also, proton pump inhibitors, such as LAN, displayed synergistic interactions with ITZ. Interestingly, FLU displayed both synergistic and antagonistic activities against ITZ-R and ITZ-S strains at the same time (Fig. 1).

(ii) Greco model. The model failed to fit the data for all combinations tested except ITZ and NIF. The program failed to fit the data in eight cases for ITZ and AMD, 13 cases for ITZ and AML, 10 cases for ITZ and LAN, 10 cases for ITZ and LID, 12 cases for ITZ and FLU, and all cases for ITZ and VER.

In the case of ITZ and NIF, α values ranged from 14.4 to 0.06; R^2 values ranged from 0.84 to 0.97 for ITZ-S strains. For the ITZ-R strains α was 8.21 (range, 0.06 to 62.7) and R^2 values ranged from 0.97 to 0.69.

(iii) Semiparametric model of Bliss. In the case of the semiparametric approach the program failed to fit the data from all data analyzed for ITZ and AMD on four occasions, with R^2

TABLE 4. In vitro interaction between ITZ and FLU[a]

Strain	MIC (μg/ml) alone		Result according to theory						
			LA				BI (nonparametric)		
			MIC (μg/ml) in combination		Result				
	ITZ	FLU	ITZ	FLU	FICI	INT	ΣSYN (*n*)	ΣANT (*n*)	INT
V09-22	0.12	160	0.06	2.5	0.52	NI	136 (36)	−125 (34)	SYN/ANT
V09-23	0.25	80	0.03	40	0.62	NI	127 (18)	−109 (22)	SYN/ANT
AZN5161	0.12	20	0.06	2.5	0.63	NI	103 (25)	−103 (21)	SYN/ANT
AZN7820	0.12	40	0.06	2.5	0.56	NI	196 (26)	−109 (24)	SYN/ANT
AZN8248	0.12	160	0.03	40	0.5	SYN	146 (25)	−168 (28)	SYN/ANT
AZN9339	0.12	80	0.12	80	2	NI	138 (27)	−106 (43)	SYN/ANT
AZN9362	0.12	40	0.12	40	2	NI	137 (24)	−151 (45)	SYN/ANT
Median	0.12	80			0.62		137	−109	
V09-18	32	40	0.12	80	2	NI	143 (57)	−150 (13)	SYN/ANT
V09-19	32	40	0.5	20	0.52	NI	134 (47)	−161 (23)	SYN/ANT
AZN5241	32	10	16	20	2.5	NI	100 (16)	−131 (24)	SYN/ANT
AZN5242	32	20	16	40	2.5	IND	188 (25)	−138 (28)	SYN/ANT
AZN7720	32	160	8	10	0.31	SYN	195 (36)	−178 (34)	SYN/ANT
AZN7722	32	160	1	10	0.09	SYN	304 (26)	−211 (24)	SYN/ANT
AZG7	32	20	8	2.5	0.38	SYN	125 (41)	−165 (39)	SYN/ANT
Median	32	40			0.52		143	−161	

[a] Abbreviations: LA, Loewe additivity; INT, interpretation; NI, no interaction; SYN, synergism; ANT, antagonism; *n*, number of interactions.

values ranging from 0.06 to 0.98 for ITZ and from −0.37 to 0.81 for AMD. The program failed to fit the data from all data analyzed for ITZ and AML on seven occasions, with R^2 values ranging from 0.009 to 0.98 for ITZ and from 0.002 to 0.75 for AML. The data could not be fitted for the combination of ITZ and LAN on two occasions, with R^2 values ranging from 0.32 to 0.99 for ITZ and from 0.002 to 0.8 for LAN. In the case of the combination of ITZ and LID, the data could not be fitted on six occasions to obtain the IC_{50}s, whereas for the other instances R^2 values ranged from 0.18 to 0.99 for ITZ and from 0.06 to 0.69 for LID. In the case of the combination of ITZ and VER, IC_{50}s could not be calculated on six occasions, with R^2 values ranging from 0.07 to 0.99 for ITZ and from −2.5 to 0.89 for VER.

IC_{50}s were calculated for the combination of ITZ and NIF and the combination of ITZ and FLU for all strains, with R^2 values ranging from 0.53 to 0.99 for ITZ, 0.58 to 0.80 for NIF, 0.22 to 0.89 for ITZ, and 0.65 to 0.92 for FLU.

DISCUSSION

Efflux mechanisms have been described in mammalian cells. In particular, the upregulation of P glycoproteins, which belong to METs of the ABC superfamily, is characteristic of cancer cells resistant to cytotoxic agents. Several investigators have reported the inhibition of these proteins with different classes of drugs in multiresistant cancer cells (45). A similar experimental principle had already been investigated to reverse chloroquine resistance in *Plasmodium falciparum* (4, 5) or the resistance to quinolone antibiotics in *Staphylococcus aureus* (27). The present study sought to investigate the effectiveness of several combinations of ITZ with MET inhibitors and nonantimicrobial membrane-active compounds, such as antiarrhythmic agents and proton pump inhibitors. We observed that some of these compounds exhibit potent antifungal effects when used in combination with ITZ.

AMD is the most complicated antiarrhythmic drug ever discovered. It has a number of electrophysiological effects that probably contribute to its antiarrhythmic effect. The drug is available for both oral and intravenous use. The peak concentration of this drug in plasma is 0.5 to 2.5 μg/ml (28), but in its steady state, the partition coefficient has been estimated to be from 100 to greater than 1,000 times higher in tissues relative to that in plasma (38). It was previously demonstrated (9, 10) that this drug alone has in vitro activity against *Aspergillus*, *Fusarium*, *Cryptococcus*, and *Candida*. We observed that the combination of this drug with ITZ showed synergistic activity against the ITZ-R strains, independent of the model used to characterize the interaction. There is as yet no explanation why this combination interacts synergistically, but the interaction could be due to the inhibition of major pumps, including efflux pumps or the calmodulin system. The concentration at which the synergistic interaction was observed is achievable in serum and tissues, and no major drug-drug interaction with ITZ has been observed in patients; therefore, the potential of this combination warrants further studies with in vivo models.

AMD, which is widely used clinically for its diuretic effect, has been recognized as a drug that possesses growth-inhibitory activity against bacterial cells (15–17).

This agent is an inhibitor of various sodium transporters and is toxic to *Schizosaccharomyces pombe* at low concentrations (19). In this study no antifungal activity of this drug alone was observed. Also, no significant interaction between ITZ and AMD against ITZ-S and ITZ-R strains was found.

One new antifungal target could be the fungal plasma membrane H^+-ATPase, which is an ATP-dependent proton pump. It plays a critical role in fungal cell physiology by regulating the intracellular pH, maintaining ionic balance, and generating the electrochemical proton gradient necessary for nutrient uptake (49, 50). The H^+-ATPase from *Saccharomyces cerevisiae* has been shown to be essential by gene-disruption experiments (50), and it displays a number of biochemical and genetic properties that make it attractive as a drug discovery target (41). The pumps mentioned above are present also in *A. fumigatus* (6). These pumps can be blocked by different compounds, including the novel compound conjugated styryl ketone, which was shown to be active when it was tested against *A. fumigatus* in vitro and in vivo (34, 35); but no drug combination was tested against *Aspergillus* in those studies. Proton pump inhibitors such as LAN and omeprazole were useful when they were used in combination with amoxicillin or erythromycin against *Helicobacter pylori* (40), and clinical evidence also indicates that these combinations are active when they are used against this pathogen in humans (31, 32). LAN is a novel benzimidazole proton pump inhibitor. Inhibition of *C. albicans* growth in vitro was demonstrated previously (3). In our study this drug alone was inactive against *A. fumigatus*, but a synergistic interaction against ITZ-R *A. fumigatus* strains was observed when it was combined with ITZ.

The mechanism of action of LAN is not clear. However, transmission electron microscopy revealed that exposure of eukaryotic cells to this drug resulted in the formation of free membranous vesicles and collapse of the cell surface structure, suggesting an effect on the cell membrane (22). These effects could contribute to the observed interaction of LAN and ITZ against ITZ-R *A. fumigatus* strains, although the explanation for the synergism remains unclear.

NIF, a calcium entry blocker, is used for the treatment of angina pectoris and arterial hypertension. In recent years it was demonstrated that some calmodulin inhibitors such as cyclosporine and tacrolimus exert antifungal activities and potentiate the actions of azoles in vitro and in animal models (33, 36, 37). Our data suggest a potent synergistic effect of NIF and ITZ against ITZ-R strains at clinically therapeutic levels (2). This effect was also observed against *C. albicans* when NIF or nimodipine was combined with ketoconazole (29, 30). This effect can be due to the fact that calcium and its binding protein, calmodulin, are known to modulate proliferation, differentiation, and metabolism in a variety of cell types. Calmodulin is a small acidic Ca^{2+} binding protein, which is thought to induce intracellular Ca^{2+} fluxes into cellular responses (8). The concentration of free intracellular calcium can be increased in eukaryotic cells by opening of the voltage-dependent calcium channels (VDCCs), allowing extracellular Ca^{2+} to enter the cell. Several chemically distinct classes of organic compounds share the ability to inhibit calcium influx through VDCCs (24). VDCCs are present in yeasts (7, 23, 54).

FLU, a phenothiazine neuroleptic, is widely used for the treatment of psychotic illnesses (1), and when it is used alone it displays activity against *C. albicans* (20). Our results suggest

that this drug exhibits antifungal activity at high concentrations. In combination with ITZ there is a paradoxical effect, in which the combination showed different interactions. This effect can be explained by the fact that FLU both turns off and induces efflux pumps, especially CDR1 (*Candida* drug resistance) and CDR2 (20), at different concentrations. FLU antagonized the activity of ITZ, especially at low concentrations of both drugs (Fig. 1), an effect that reflects the induction of pumps and the reduction of the activities of the azoles. On the contrary, at high concentrations the antagonistic activity was reproducibly replaced by a synergistic interaction. This effect has also been demonstrated against *C. albicans* by agar techniques and molecular methods (20).

In this study, the data could not satisfactorily be fitted to the Greco model. This may well be explained by the fact that one of the two drugs in the combinations tested does not follow a sigmoid dose-response, and consequently, the IC_{50} and the fit of the data obtained cannot be points, because each drug by itself showed no antifungal effect. In this case nonparametric approaches are more useful.

ITZ is metabolized predominantly by the cytochrome P450 3A4 isoenzyme system; and concomitant administration with dihydropyridines, such as NIF, results in increasing concentrations of these drugs in plasma. Side effects such as edema might occur if appropriate dose adjustments are not made (51). Concomitant administration of ITZ capsules with proton pump inhibitors may cause reduced concentrations of the azole in plasma because of decreased absorption and may be associated with treatment failure (25). Administration of the oral solution or intravenous formulation may overcome this problem (26).

In conclusion, this is the first study in which the activity of ITZ in combination with nonantibacterial membrane-active compounds was investigated against *A. fumigatus*. Further studies are needed to understand the mechanisms underlying the observed synergistic interaction and are warranted in order to develop new therapeutic strategies for the treatment of invasive aspergillosis.

REFERENCES

1. **Aravagiri, M., S. R. Marder, A. Yuwiler, K. K. Midha, N. S. Kula, and R. J. Baldessarini.** 1995. Distribution of fluphenazine and its metabolites in brain regions and other tissues of the rat. Neuropsychopharmacology **13:**235–247.
2. **Benet, L. Z., O. Svein, and J. B. Schwartz.** 1996. Design and optimization of dosage regimens; pharmacokinetics data, p. 1765. *In* P. Molinoff, R. Ruddon, and A. Goodman Gilman (ed.), Goodman & Gilman's the pharmacological basis of therapeutics, 9th ed. McGraw-Hill, New York, N.Y.
3. **Biswas, S. K., K. Yokoyama, K. Kamei, K. Nishimura, and M. Miyaji.** 2001. Inhibition of hyphal growth of *Candida albicans* by activated lansoprazole, a novel benzimidazole proton pump inhibitor. Med. Mycol. **39:**283–285.
4. **Bitonti, A. J., and P. P. McCann.** 1989. Desipramine and cyproheptadine for reversal of chloroquine resistance in *Plasmodium falciparum.* Lancet **ii:**1282–1283.
5. **Bitonti, A. J., A. Sjoerdsma, P. P. McCann, D. E. Kyle, A. M. Oduola, R. N. Rossan, W. K. Milhous, and D. E. Davidson, Jr.** 1988. Reversal of chloroquine resistance in malaria parasite *Plasmodium falciparum* by desipramine. Science **242:**1301–1303.
6. **Burghoorn, H. P., P. Soteropoulos, P. Paderu, R. Kashiwazaki, and D. S. Perlin.** 2002. Molecular evaluation of the plasma membrane proton pump from *Aspergillus fumigatus.* Antimicrob. Agents Chemother. **46:**615–624.
7. **Catterall, W. A.** 1998. Yeasty brew yields novel calcium channel inhibitor. Nat. Biotechnol. **16:**906.
8. **Cheung, W. Y.** 1980. Calmodulin plays a pivotal role in cellular regulation. Science **207:**19–27.
9. **Courchesne, W. E.** 2002. Characterization of a novel, broad-based fungicidal activity for the antiarrhythmic drug amiodarone. J. Pharmacol. Exp. Ther. **300:**195–199.
10. **Courchesne, W. E., and S. Ozturk.** 2003. Amiodarone induces a caffeine-inhibited, MID1-dependent rise in free cytoplasmic calcium in *Saccharomyces cerevisiae.* Mol. Microbiol. **47:**223–234.
11. **Denning, D. W., R. M. Tucker, L. H. Hanson, and D. A. Stevens.** 1989. Treatment of invasive aspergillosis with itraconazole. Am. J. Med. **86:**791–800.
12. **Denning, D. W., K. Venkateswarlu, K. L. Oakley, M. J. Anderson, N. J. Manning, D. A. Stevens, D. W. Warnock, and S. L. Kelly.** 1997. Itraconazole resistance in *Aspergillus fumigatus.* Antimicrob. Agents Chemother. **41:**1364–1368.
13. **De Waard, M. A., and J. G. Van Nistelrooy.** 1981. Induction of fenarimol-efflux activity in *Aspergillus nidulans* by fungicides inhibiting sterol biosynthesis. J. Gen. Microbiol. **126:**483–489.
14. **Drusano, G. L., D. Z. D'Argenio, W. Symonds, P. A. Bilello, J. McDowell, B. Sadler, A. Bye, and J. A. Bilello.** 1998. Nucleoside analog 1592U89 and human immunodeficiency virus protease inhibitor 141W94 are synergistic in vitro. Antimicrob. Agents Chemother. **42:**2153–2159.
15. **Giunta, S., L. Galeazzi, G. Turchetti, G. Grilli, and G. Groppa.** 1988. *Streptococcus faecalis* susceptibility to amiloride depends on medium pH. Pharmacol. Res. Commun. **20:**853–861.
16. **Giunta, S., L. Galeazzi, G. Turchetti, G. Sampaoli, and G. Groppa.** 1986. Effect of amiloride on the intracellular sodium and potassium content of intact *Streptococcus faecalis* cells in vitro. Antimicrob. Agents Chemother. **29:**958–959.
17. **Giunta, S., C. Pieri, and G. Groppa.** 1984. Amiloride, a diuretic with in vitro antimicrobial activity. Pharmacol. Res. Commun. **16:**821–829.
18. **Greco, W. R., G. Bravo, and J. C. Parsons.** 1995. The search for synergy: a critical review from a response surface perspective. Pharmacol. Rev. **47:**331–385.
19. **Haworth, R. S., E. J. Cragoe, Jr., and L. Fliegel.** 1993. Amiloride and 5-(*N*-ethyl-*N*-isopropyl) amiloride inhibit medium acidification and glucose metabolism by the fission yeast *Schizosaccharomyces pombe.* Biochim. Biophys. Acta **1145:**266–272.
20. **Henry, K. W., M. C. Cruz, S. K. Katiyar, and T. D. Edlind.** 1999. Antagonism of azole activity against *Candida albicans* following induction of multidrug resistance genes by selected antimicrobial agents. Antimicrob. Agents Chemother. **43:**1968–1974.
21. **Hindler, J.** 1995. Antimicrobial susceptibility testing, p. 5.18.11–15.18.20. *In* H. D. Eisenberg (ed.), Clinical microbiology procedures handbook. American Society for Microbiology, Washington, D.C.
22. **Iwahi, T., H. Satoh, M. Nakao, T. Iwasaki, T. Yamazaki, K. Kubo, T. Tamura, and A. Imada.** 1991. Lansoprazole, a novel benzimidazole proton pump inhibitor, and its related compounds have selective activity against *Helicobacter pylori.* Antimicrob. Agents Chemother. **35:**490–496.
23. **Jan, L. Y., and Y. N. Jan.** 1989. Voltage-sensitive ion channels. Cell **56:**13–25.
24. **Janis, R. A., and D. J. Triggle.** 1983. New developments in Ca^{2+} channel antagonists. J. Med. Chem. **26:**775–785.
25. **Jaruratanasirikul, S., and S. Sriwiriyajan.** 1998. Effect of omeprazole on the pharmacokinetics of itraconazole. Eur. J. Clin. Pharmacol. **54:**159–161.
26. **Johnson, M. D., C. D. Hamilton, R. H. Drew, L. L. Sanders, G. J. Pennick, and J. R. Perfect.** 2003. A randomized comparative study to determine the effect of omeprazole on the peak serum concentration of itraconazole oral solution. J. Antimicrob. Chemother. **51:**453–457.
27. **Kaatz, G. W., and S. M. Seo.** 1995. Inducible NorA-mediated multidrug resistance in *Staphylococcus aureus.* Antimicrob. Agents Chemother. **39:**2650–2655.
28. **Kowey, P. R., R. A. Marinchak, S. J. Rials, and D. Bharucha.** 1997. Pharmacologic and pharmacokinetic profile of class III antiarrhythmic drugs. Am. J. Cardiol. **80:**16G–23G.
29. **Krajewska-Kulak, E., and W. Niczyporuk.** 1993. Effects of the combination of ketoconazole and calcium channel antagonists against *Candida albicans* in vitro. Arzneimittelforschung **43:**782–783.
30. **Krajewska-Kulak, E., and W. Niczyporuk.** 1993. Effects of the combination of ketoconazole and calmodulin inhibitors against *Candida albicans* in vitro. Arzneimittelforschung **43:**1018–1019.
31. **Logan, R. P., P. A. Gummett, B. T. Hegarty, M. M. Walker, J. H. Baron, and J. J. Misiewicz.** 1992. Clarithromycin and omeprazole for *Helicobacter pylori.* Lancet **340:**239.
32. **Logan, R. P., P. A. Gummett, H. D. Schaufelberger, R. R. Greaves, G. M. Mendelson, M. M. Walker, P. H. Thomas, J. H. Baron, and J. J. Misiewicz.** 1994. Eradication of *Helicobacter pylori* with clarithromycin and omeprazole. Gut **35:**323–326.
33. **Maesaki, S., P. Marichal, M. A. Hossain, D. Sanglard, H. Vanden Bossche, and S. Kohno.** 1998. Synergic effects of tacrolimus and azole antifungal agents against azole-resistant *Candida albicans* strains. J. Antimicrob. Chemother. **42:**747–753.
34. **Manavathu, E. K., J. R. Dimmock, S. C. Vashishtha, and P. H. Chandrasekar.** 1999. Proton-pumping-ATPase-targeted antifungal activity of a novel conjugated styryl ketone. Antimicrob. Agents Chemother. **43:**2950–2959.
35. **Manavathu, E. K., J. R. Dimmock, S. C. Vashishtha, J. Cutright, and P. H. Chandrasekar.** 1998. In-vitro and in-vivo susceptibility of *Aspergillus fumiga-*

tus to a novel conjugated styryl ketone. J. Antimicrob. Chemother. **42:**585–590.
36. **Marchetti, O., J. M. Entenza, D. Sanglard, J. Bille, M. P. Glauser, and P. Moreillon.** 2000. Fluconazole plus cyclosporine: a fungicidal combination effective against experimental endocarditis due to *Candida albicans.* Antimicrob. Agents Chemother. **44:**2932–2938.
37. **Marchetti, O., P. Moreillon, M. P. Glauser, J. Bille, and D. Sanglard.** 2000. Potent synergism of the combination of fluconazole and cyclosporine in *Candida albicans.* Antimicrob. Agents Chemother. **44:**2373–2381.
38. **Mason, J. W.** 1987. Amiodarone. N. Engl. J. Med. **316:**455–466.
39. **Meletiadis, J., J. W. Mouton, J. F. Meis, and P. E. Verweij.** 2003. In vitro drug interaction modeling of combinations of azoles with terbinafine against clinical *Scedosporium prolificans* isolates. Antimicrob. Agents Chemother. **47:**106–117.
40. **Midolo, P. D., J. D. Turnidge, and J. R. Lambert.** 1997. Bactericidal activity and synergy studies of proton pump inhibitors and antibiotics against *Helicobacter pylori* in vitro. J. Antimicrob. Chemother. **39:**331–337.
41. **Monk, B. C., and D. S. Perlin.** 1994. Fungal plasma membrane proton pumps as promising new antifungal targets. Crit. Rev. Microbiol. **20:**209–223.
42. **Moore, C. B., N. Sayers, J. Mosquera, J. Slaven, and D. W. Denning.** 2000. Antifungal drug resistance in *Aspergillus.* J. Infect. **41:**203–220.
43. **National Committee for Clinical Laboratory Standards.** 2002. Reference method for broth dilution antifungal susceptibility testing of conidium-forming filamentous fungi; approved standard. Document M-38A. National Committee for Clinical Laboratory Standards, Wayne, Pa.
44. **Odds, F. C.** 2003. Synergy, antagonism, and what the chequerboard puts between them. J. Antimicrob. Chemother. **52:**1.
45. **Pastan, I., and M. Gottesman.** 1987. Multiple-drug resistance in human cancer. N. Engl. J. Med. **316:**1388–1393.
46. **Prichard, M. N., L. E. Prichard, and C. Shipman, Jr.** 1993. Strategic design and three-dimensional analysis of antiviral drug combinations. Antimicrob. Agents Chemother. **37:**540–545.
47. **Prichard, M. N., and C. Shipman, Jr.** 1990. A three-dimensional model to analyze drug-drug interactions. Antivir. Res. **14:**181–205.
48. **Sanglard, D., K. Kuchler, F. Ischer, J. L. Pagani, M. Monod, and J. Bille.** 1995. Mechanisms of resistance to azole antifungal agents in *Candida albicans* isolates from AIDS patients involve specific multidrug transporters. Antimicrob. Agents Chemother. **39:**2378–2386.
49. **Serrano, R.** 1988. H^+-ATPase from plasma membranes of *Saccharomyces cerevisiae* and *Avena sativa* roots: purification and reconstitution. Methods Enzymol. **157:**533–544.
50. **Serrano, R., M. C. Kielland-Brandt, and G. R. Fink.** 1986. Yeast plasma membrane ATPase is essential for growth and has homology with (Na^+ + K^+), K^+- and Ca^{2+}-ATPases. Nature **319:**689–693.
51. **Tailor, S. A., A. K. Gupta, S. E. Walker, and N. H. Shear.** 1996. Peripheral edema due to nifedipine-itraconazole interaction: a case report. Arch. Dermatol. **132:**350–352.
52. **Te Dorsthorst, D. T., P. E. Verweij, J. F. Meis, N. C. Punt, and J. W. Mouton.** 2002. Comparison of fractional inhibitory concentration index with response surface modeling for characterization of in vitro interaction of antifungals against itraconazole-susceptible and -resistant *Aspergillus fumigatus* isolates. Antimicrob. Agents Chemother. **46:**702–707.
53. **Te Dorsthorst, D. T., P. E. Verweij, J. Meletiadis, M. Bergervoet, N. C. Punt, J. F. Meis, and J. W. Mouton.** 2002. In vitro interaction of flucytosine combined with amphotericin B or fluconazole against thirty-five yeast isolates determined by both the fractional inhibitory concentration index and the response surface approach. Antimicrob. Agents Chemother. **46:**2982–2989.
54. **Tomaselli, G. F., P. H. Backx, and E. Marban.** 1993. Molecular basis of permeation in voltage-gated ion channels. Circ. Res. **72:**491–496.